

# All Tied Up: An Introduction to Knot Theory

Grace Belmonte, Finlay Dowds  
Jake Hopper, Sophie Worsfold

November 26, 2024

## Abstract

Knot theory is at the cutting edge of mathematics research. In this paper, we outline the fundamentals of knots and describe concepts of equivalence and invariance before looking into knot theory's topological roots. We conclude by exploring the scientific significance of knots in molecular chemistry and protein biology.

## Contents

<b>1</b>	<b>Introduction</b>	<b>2</b>
<b>2</b>	<b>Fundamentals</b>	<b>2</b>
2.1	Notation . . . . .	3
2.2	Key Knots . . . . .	3
2.3	Composite and Prime Knots . . . . .	4
2.4	Links . . . . .	5
2.5	Tangles . . . . .	6
<b>3</b>	<b>The Knot Equivalence Problem</b>	<b>7</b>
3.1	Reidemeister Moves . . . . .	7
3.2	Tricolourability . . . . .	9
3.3	Determinant and p-colourability . . . . .	11
<b>4</b>	<b>Knot Polynomials</b>	<b>15</b>
4.1	The Alexander Polynomial . . . . .	15
4.2	The Jones Polynomial . . . . .	18
<b>5</b>	<b>Categorisation of Knots from a Topological Perspective</b>	<b>21</b>
5.1	Torus Knots . . . . .	21
5.2	Satellite Knots . . . . .	23
5.3	Hyperbolic Knots . . . . .	25
<b>6</b>	<b>Applications of Knot Theory Within Chemistry and Biology</b>	<b>27</b>
6.1	Molecular Chirality . . . . .	28
6.2	Protein Folding . . . . .	33

<b>7 Conclusion</b>	<b>38</b>
<b>References</b>	<b>39</b>
<b>Appendix</b>	<b>43</b>

## 1 Introduction

In 1867, Lord Kelvin attended a demonstration of the properties of smoke rings by fellow physicist Peter Guthrie Tait. Kelvin theorised that different atoms were formed from distinct knotted structures of aether, and that perhaps knots were fundamental to the very world around us. This inspired Tait to tabulate as many knots as he could, with the hope that he would be constructing the very first periodic table. Kelvin and Tait were wrong, of course, and by the end of the 19<sup>th</sup> century, chemists and physicists all but lost interest in knots. But mathematicians were hooked.

Throughout the 20<sup>th</sup> century, leading topologists turned their hands to knot theory. Henri Poincaré, Max Dehn and Kurt Reidemeister (whom we will hear from in Section 3) left their mark on knot theory before Thurston and Jones each came to win Fields medals for their work on knots in 1982 and 1990, respectively. In the 1980s, biologists discovered knotting in DNA, and chemists found that knotting molecules controlled key physical and chemical properties around the same time. This took the mathematical community by surprise; such an abstract area of maths, so removed from practical application, had found its place in the physical world. Now supported by vast computing power, mathematicians today continue to explore knot theory, once again searching for knots in the structure of our world, almost two hundred years after Lord Kelvin and Peter Guthrie Tait first stepped into the world of knot theory.

## 2 Fundamentals

Having explored the history of knot theory, we now turn our attention to its foundations. First, we will consider the formal definition of a knot.

**Definition 2.1** (Knot). A knot  $K \subset \mathbb{R}^3$  is a subset of points homeomorphic to a circle.

However, this definition is somewhat vague and so we will note the more physical approach described by Adams in his prominent book on knot theory, *The Knot Book* [1]. In fact, Adams' work is so integral to knot theory that our project largely follows it.

His approach involves first taking a piece of string and then tying a knot in it. Next, connect both ends of the string to create a closed loop. For a string with zero thickness, this is what is known as a **mathematical knot**.

Interestingly, two knots are equivalent if we can **smoothly deform** one to create the other. By this, we mean not allowing a piece of the knot to be reduced

to a point. Instead, the deformation must resemble the continuous manipulation that would be possible with our piece of string.

## 2.1 Notation

Whilst there are many ways to denote a given knot, we will refer to a knot by either what it is commonly known as, or its **Alexander-Briggs notation** [2]. This type of notation was first devised in 1926 and is accepted by knot theorists as being the standard way to tabulate knots.

By smoothly deforming a knot, it is possible to achieve a representation of a knot (called a **projection**) that consists of the fewest possible crossings. This gives the **minimal crossing number**, which is used to categorise a knot. Together with an arbitrary subscript (taken from the tabulations made by Tait in the 19<sup>th</sup> century [3]), we can write the Alexander-Briggs notation of a given knot,  $K$ , as  $N_i$ , where  $N$  is the minimal crossing number and  $i$  is the specific subscript from Tait's tabulations.

## 2.2 Key Knots

We now give several key knots along with their respective Alexander-Briggs notations, which will frequently reappear throughout the subsequent sections.

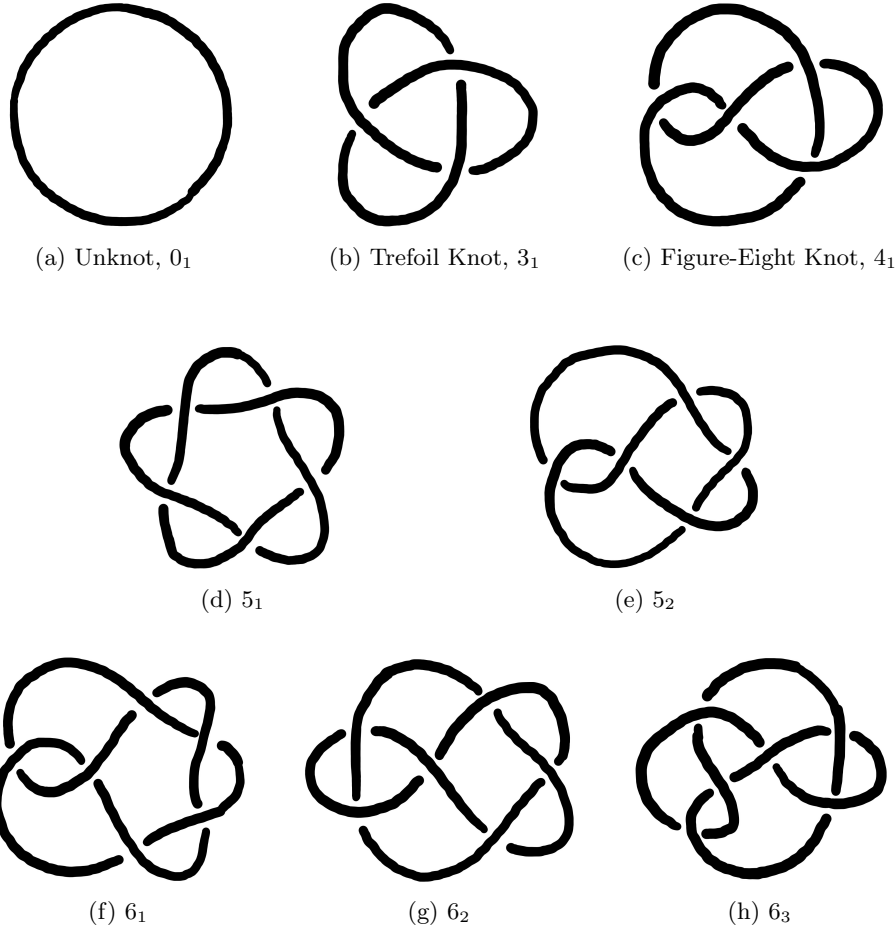


Figure 1: A selection of knots with their Alexander-Briggs notation. The first three knots include their common names alongside the notation.

### 2.3 Composite and Prime Knots

From the knots shown above in Figure 1, and indeed from any other knots, it is possible to construct new knots.

**Definition 2.2** (Connected Sum). If  $K_1$  and  $K_2$  are knots, their connected sum, denoted  $K = K_1 \# K_2$ , is formed by:

- (1) removing a small arc from each knot, chosen to be on the outside of both projections and avoiding any crossings, and then
- (2) connecting the cut ends with straight arcs that do not cross the projection.

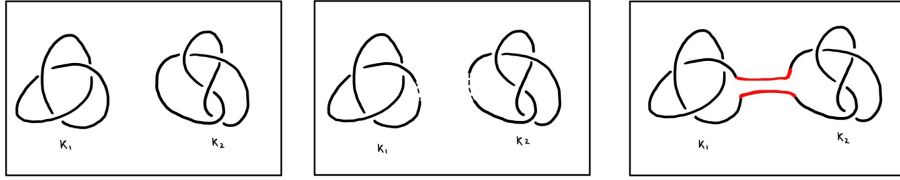


Figure 2: The connected sum of two knots,  $K_1$  and  $K_2$ .

We say a knot,  $K$ , is **composite** if there exist **non-trivial knots**  $K_1$  and  $K_2$  such that  $K = K_1 \# K_2$ . By a non-trivial knot, we make clear we mean any knot other than the unknot (Image 1a in Figure 1), which is the knot that has no crossings.

As one might expect, the composition of knots is not unique; two knots can together yield many different compositions. After all, we can choose which arcs to select for removal from the two knots in our construction of their connected sum, and different choices give rise to different composite knots.

It should also not come as much of a surprise that knot composition lends itself naturally to the defining of **prime knots**. Analogous to how prime numbers are defined in number theory, we say a knot,  $K$ , is prime if it is not composite (i.e., if the only composition of  $K$  is of itself and the unknot). All the knots making up our catalogue of key knots in Figure 1 are considered prime, but to prove this is arduous, as the primary method is to systematically eliminate potential compositions through trial and error [3].

## 2.4 Links

However, we can also compose knots in a different way - through links.

**Definition 2.3** (Link). A link  $L$  is a finite disjoint union of knots  $K_i$ , represented as  $L = K_1 \cup \dots \cup K_n$ . Each knot  $K_i$  is called a **component** of the link, and the total number of components is referred to as the **multiplicity** of a link and is denoted by  $\mu(L)$ .

Intuitively, a link can be thought of as ‘tangling up’ some knots together. A link can be considered **splittable** if its components can be drawn without any crossings between them. And so, we note every individual knot can be categorised as a link that has only a single component.

In Figure 3 below, we present three distinct links that are all composed of only the unknot and are each **unsplittable** (i.e., not splittable). For the reader’s own understanding, we will say here that both the Whitehead and Hopf links have multiplicity  $\mu(L) = 2$  while the Borromean rings has multiplicity  $\mu(L) = 3$ . This distinction should be apparent.

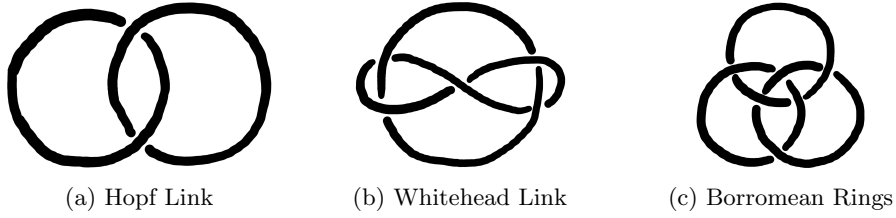


Figure 3: Three key links.

## 2.5 Tangles

Tangles describe how a knot behaves in a specific region, and give rise to another method of constructing new knots.

**Definition 2.4** (Tangle). A tangle is a region of a knot surrounded by a circle such that the knot crosses the circle exactly four times.

In Definition 2.4 above, these crossings are often thought of as occurring at the cardinal directions: north-west, north-east, south-west, and south-east. It is worth noting that, unlike knots, there is not one single ‘untangle’ but rather two simplest tangles. They are denoted as the  $\infty$ -tangle and the 0-tangle, and are as shown in Figure 4 below.

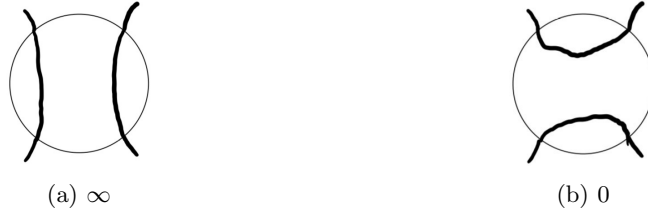


Figure 4: The two simplest tangles.

Tangles can also be used as a way to obtain new knots. For this to be done, we only change a certain tangle within a knot.

**Definition 2.5** (Mutation). A mutation is an operation in which we extract a tangle from inside a knot and either rotate it  $180^\circ$  or reflect it, horizontally or vertically. A knot obtained through a mutation is called a **mutant** of the original knot.

In Figure 5 below, we present an example of a pair of knots related by mutation called the Kinoshita-Terasaka Mutants. These are covered in more detail in [1].

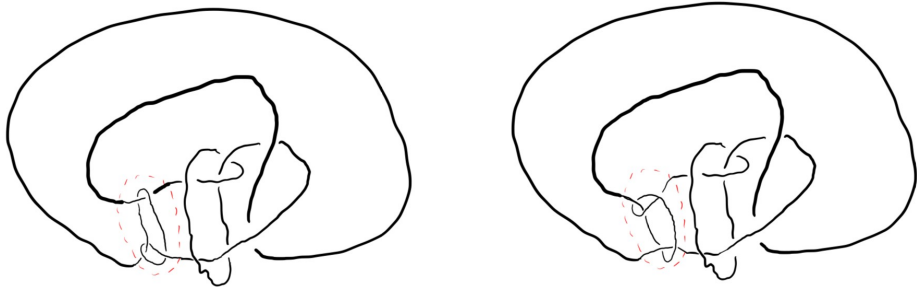


Figure 5: A pair of mutant knots.

Later, we will see an intriguing characteristic of mutants knots in Section 5.3, as well as an important use of tangles in Section 4.2. But, before then, we will first use our burgeoning understanding of how knots work to look into the knot equivalence problem.

### 3 The Knot Equivalence Problem

Before we begin, it is important to note that Sections 3.1 and 3.2 are heavily based on Adams' *The Knot Book* [1].

#### 3.1 Reidemeister Moves

The fundamental question of knot theory is how we can tell if two knots are the same. Unfortunately, this is deceptively tricky. The main motivation for this is that knot theorists have been trying to tabulate increasingly complex prime knots (as defined in Section 2.3) for centuries. In order to do this, we need to be able to tell whether two knots are actually distinct.

With us having earlier seen in Section 2 how two projections are the same knot if it is possible to smoothly deform one to create the other, we are now going to take a more rigorous approach to this idea.

**Definition 3.1** (Reidemeister Move). A Reidemeister move is a transformation of a knot projection that changes the relation between crossings. We have three types:

- (1) Adding or taking away a loop,
- (2) Adding or removing two crossings,
- (3) Sliding a strand over a crossing.

We call a smooth deformation that does not change the relation between crossings a **planar isotopy**.

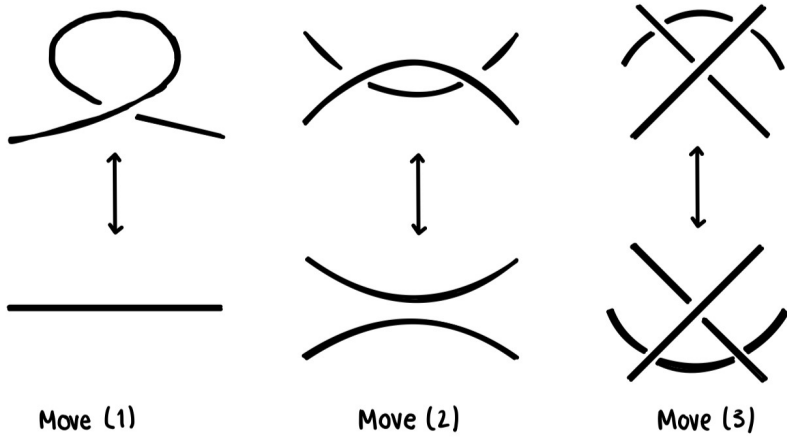


Figure 6: The three types of Reidemeister move.

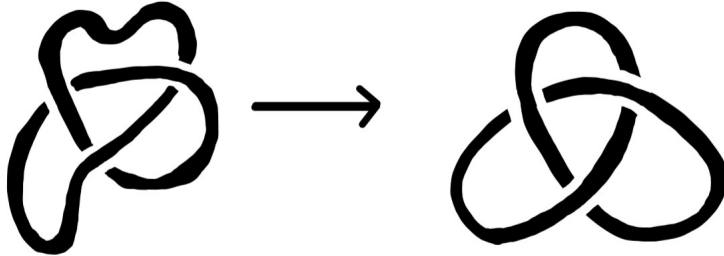


Figure 7: A planar isotopy.

**Theorem 3.2.** *We can transform one projection of a knot to another using only Reidemeister moves and planar isotopies.*

This important theorem was proved by Reidemeister in 1926 [4]. Its proof is beyond the scope of this project, but the statement itself is integral to us. With it in our arsenal, we can now be sure that two knots are the same if we are able to find some sequence of Reidemeister moves to get from one to the other.

**Example 3.1.**

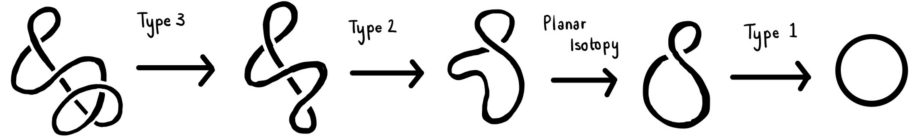


Figure 8: Using Reidemeister moves to show equivalence to the unknot.

In Figure 8 above, we have been able to show that a seemingly complicated knot is actually just the unknot through the use of all three Reidemeister moves (Figure 6) and a planar isotopy (Figure 7).

### 3.2 Tricolourability

Given all of the knot theory we have learnt so far, it might be a surprise to know that we still have not actually *proved* that there is more than one knot in existence.

Think of it this way: while we cannot use Reidemeister moves to transform the trefoil knot into the unknot, we do not yet know that this is impossible. In fact, even if we showed that this transformation could not be done in one thousand Reidemeister moves, what is to say it could not be done in two thousand? To combat this, we need a way of telling whether two knots are different.

**Definition 3.3** (Invariant). An invariant is some characteristic of a knot that is the same for every projection.

The simplest of these would be a knot's minimal crossing number (mentioned in Section 2.1). However, this is not a very useful invariant because, in order to show a knot has a minimal crossing number greater than zero, we would have to show that it is not the unknot, which we cannot yet do. The following definition should help us in this regard.

**Definition 3.4** (Tricolourable). We call a **strand** a piece of a knot that goes from under-crossing to under-crossing, with only over-crossings in between. As their names suggest, an **under-crossing** is a point where one strand passes under another in a projection while an **over-crossing** is a point where one strand passes over another.

We call a knot tricolourable if we can colour each strand one of three colours such that at each crossing either:

- (1) all three different colours come together, or
- (2) all of the same colour comes together.

We also require that at least two colours are used in the colouring.

**Example 3.2.** We are able to demonstrate that the trefoil is tricolourable. In Figure 9 below, we can see that each crossing involves each of the three colours.

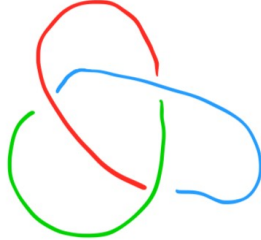


Figure 9: The trefoil coloured.

It should come as no surprise that we can combine the previous definitions to give the following theorem.

**Theorem 3.5.** *Tricolourability is an invariant.*

*Proof.* To prove this, we need to show that if one projection of a knot is tricolourable then so is every projection. However, as we can get between projections of the same knot using Reidemeister moves, we only have to show that tricolourability is constant over each type. We do this in the Figure 10.

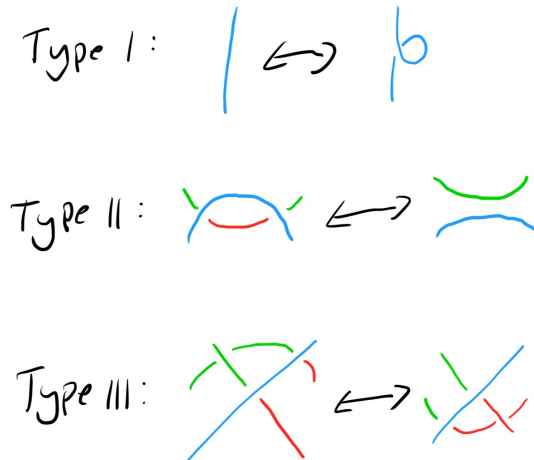


Figure 10: Tricolourability is preserved under Reidemeister moves.

There are more cases (colourings) to consider than shown in Figure 10, however they all follow very simply and so are omitted for the sake of brevity. The key point to make is that our rules for tricolourability remain consistent through all Reidemeister moves.

It is worth noting too that this then means if one projection of a knot is not tricolourable, then no projections of that knot can be tricolourable. If any projection were to be tricolourable, this would force all projections tricolourable.

□

Let us once again consider if the trefoil and the unknot are distinct. As the unknot can only be coloured with one colour, it is clearly not tricolourable and since Example 3.2 shows that the trefoil is tricolourable, we can be certain that it is not the unknot. Hence, they are different knots and so we have confirmed the existence of at least two knots.

### 3.3 Determinant and p-colourability

Before we continue on with our exploration of the knot equivalence problem, we do need to point out that we are now largely following Dixon's work in her paper from 2010 [5].

While earlier we found tricolourability to tell us that there are at least two knots, it unfortunately does not tell us anything more. This is because tricolourability is a **Boolean invariant**; a knot is either tricolourable or not tricolourable. So in order to differentiate inside these two categories of knot, we need to generalise.

**Definition 3.6** (p-colourability). We say a knot is p-colourable for some prime  $p > 2$  if we can assign each strand of the knot diagram an integer  $1, 2, \dots, p$  such that at any crossing:

$$2 \cdot O \equiv U_1 + U_2 \pmod{p},$$

where  $O$  is the integer assigned to the over-strand and  $U_1, U_2$  are the integers assigned to the under-strands. Here, an **over-strand** refers to a strand that passes 'over' the other strands at a crossing while an **under-strand** expectedly refers to a strand that passes 'under' the other strands.

Similarly to tricolourability, we also require that at least two distinct integers be used in the colouring.

**Example 3.3.** We can prove that the figure-eight knot of Image 1c in Figure 1 is 5-colourable.

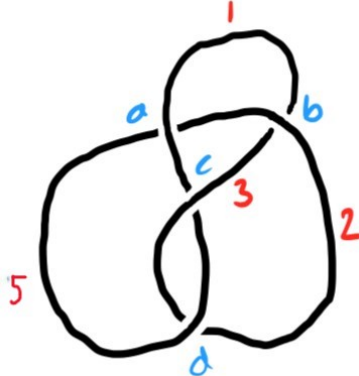


Figure 11: The figure-eight knot coloured.

Using Figure 11 together with Definition 3.6, we are able to form equations for each crossing. These are:

- For crossing  $a$ , we find  $2 \cdot 1 \equiv 2 \equiv 2 + 5 \pmod{5}$ . This is always true ✓.
- For crossing  $b$ , we find  $2 \cdot 2 \equiv 4 \equiv 1 + 3 \pmod{5}$ . This is always true ✓.
- For crossing  $c$ , we find  $2 \cdot 3 \equiv 1 \equiv 1 + 5 \pmod{5}$ . This is always true ✓.
- For crossing  $d$ , we find  $2 \cdot 5 \equiv 0 \equiv 2 + 3 \pmod{5}$ . This is always true ✓.

Hence, the figure-eight knot is 5-colourable. It is also worth noting that while we did not use the colour 4 here, this was completely acceptable to have done so because we knew as long as we were to use at least two colours, we could omit as many of the others as we wished.

From this, it is fairly intuitive to see that tricolourability is a specific case of  $p$ -colourability. If the over-strand at a crossing was 1, for example, then the sum of the under-strands would have to be such that the right side of our linear congruence equation in Definition 3.6 was  $2 \pmod{3}$ . Therefore, the two under-strands would either have to be both 1, or be 2 and 3 which gives the two cases we allow in tricolourability.

Later on in this section, as part of a stronger result, we will see for each prime  $p > 2$  that  $p$ -colourability is an invariant. Already though, a picture is starting to form. Each knot has a selection of primes  $p > 2$  for which it is  $p$ -colourable, and while each of these invariants is Boolean, by taking them together, we are able to form a single stronger invariant.

But, we unfortunately have a problem. Showing that a knot is  $p$ -colourable can be difficult, and showing that there are no other primes  $q$  such that it is ‘ $q$ -colourable’ is of even greater difficulty. Hence, we need to start thinking outside the box.

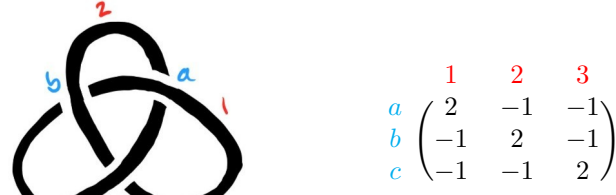
To begin to do so, we will observe that our definition of p-colourability creates a system of equations where we have one equation for each crossing. From this, we can form the colouring matrix of a knot.

**Definition 3.7** (Colouring Matrix). Label each crossing of a knot projection from  $1, \dots, n$  and do the same for the strands, noting that there are trivially the same number of each. We then form an  $n \times n$  matrix,  $M = (m_{i,j})$ , such that its elements are given by:

$$m_{i,j} = \begin{cases} 2, & \text{if } j \text{ is the over-stand of crossing } i, \\ -1, & \text{if } j \text{ is an under-strand of crossing } i, \\ 0, & \text{otherwise.} \end{cases}$$

We call the resulting matrix  $M$  the colouring matrix of the given projection.

Returning to our example of the trefoil, we can obtain the following:



(a) The trefoil knot coloured.

(b) The colouring matrix.

Figure 12: In 12a, we present the trefoil knot coloured. Then, we have proceeded to present next to it its colouring matrix in 12b.

It is important to note that we have a slight problem for a loop, such as the one encountered in the first Reidemeister move where in which a single strand forms both the over-crossing as well as one of the under-crossings. In this particular case, we assign it the value 1, which is intuitive because by right it should be both 2 and  $-1$ ; so, we simply add the two numbers [6].

Our obvious choice for turning this into an invariant would be to take the determinant. However, as our equations are linearly independent, the determinant will always be zero. Hence, we have to try something else.

**Definition 3.8** (Minor). The  $i, j$  minor of a matrix  $A$  is the determinant of the matrix obtained by removing row  $i$  and column  $j$  from  $A$ .

**Definition 3.9** (Knot Determinant). The determinant of a knot is the absolute value of any minor of its colouring matrix.

**Example 3.4.** Using our earlier colouring matrix of 12b from Figure 12, we can see that the trefoil's knot determinant is the determinant of the matrix:

$$\begin{pmatrix} 2 & -1 \\ -1 & 2 \end{pmatrix}.$$

This is irrespective of which row  $i$  and which column  $j$  we choose to remove. And so, we therefore find its determinant to be 3.

**Example 3.5.** The unknot is a more difficult case; with no crossings, we cannot form a colouring matrix. We are thereby forced to attempt to deform it to see if we can form a colouring matrix this way. Our attempt is as follows.

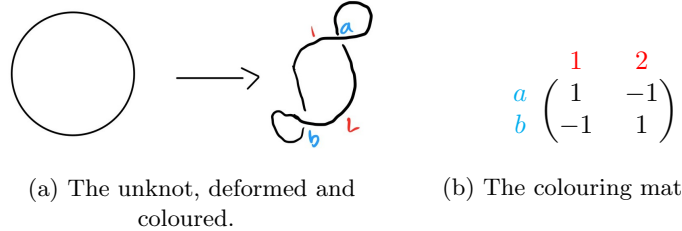


Figure 13: To find the determinant of the unknot, we start by first deforming it and presenting its deformation coloured in 13a. Then, we proceed to present the corresponding colouring matrix in 13b.

Evidently, by deforming the unknot as seen in Figure 13 we have been able to obtain its colouring matrix. Hence, we can now use Definitions 3.8 and 3.9 to tell us the unknot's knot determinant is 1.

Next, we give some important results about knot determinants.

**Proposition 3.10.** *The knot determinant is well-defined.*

*Proof.* This is proved through a linear algebra result which states that the minors of any square matrix, where the rows and columns sum to 0, are equal. Then, a result from [7] tells us we can transform a colouring matrix to have rows summing to 0 without changing the absolute value of the determinant.  $\square$

**Theorem 3.11.** *The knot determinant is an invariant.*

*Proof.* This proof is beyond the scope of this project, but it once again simply requires checking that each Reidemeister move does not alter the knot determinant. For a full proof, see [5].  $\square$

**Theorem 3.12.** *A knot  $K$  is  $p$ -colourable if and only if  $p$  divides its knot determinant.*

*Proof.* For a knot with colouring matrix  $M$  to be  $p$ -colourable, we need a non-constant solution to  $M\mathbf{v} \equiv \mathbf{0} \pmod{p}$ . Note that any constant vector will be a solution which corresponds to only using one colour. This implies that the kernel of  $M$  has dimension at least 2 (at least 1, as every constant vector works, and then we need another solution, giving a total dimension of at least 2). Hence, by the Rank-Nullity Theorem (a standard result in linear algebra), we have that  $\text{rank}(M) < n - 1$ . This forces the determinant of the minors to be  $0 \pmod{p}$ , which is exactly our statement and so [6]'s proof is complete.  $\square$

Immediately, we can apply this to Example 3.4 which gives that the trefoil knot is tricolourable but not  $p$ -colourable for any other prime  $p$ . Subsequently, we can apply Theorem 3.11 to get the following result.

**Corollary 3.13.** *For each prime  $p > 2$ ,  $p$ -colourability is an invariant.*

*Proof.* This follows immediately from Theorem 3.11 and Theorem 3.12.  $\square$

**Remark 3.14.** Knot determinants (and hence  $p$ -colourability) are related to connected sums (see Section 2.3) as we can show that for any two knots  $K_1$  and  $K_2$ , we have  $\det(K_1 \# K_2) = \det(K_1) \cdot \det(K_2)$ . For a proof of this, see [5].

So, we now have a much more specific way of differentiating knots. This is hugely helpful, but by no means a full solution to the knot equivalence problem as we have many knots that share knot determinants. We will see even more powerful invariants in Section 5.3, and we will also consider a new category of invariants in the following section.

## 4 Knot Polynomials

As mentioned, a primary aim of knot theory is to tabulate all prime knots. Our exploration of invariants thus far has been helpful; however,  $p$ -colourability is relatively weak and does not allow us to differentiate between many knots. This introduces the study of knot polynomials and how they can be defined for different knots.

There are several types of knot polynomials to utilise when studying knots. Many are straight forward, and favoured over previously stated methods. In this section, we will focus on the two most fundamental knot polynomials: the Alexander polynomial and the Jones polynomial.

### 4.1 The Alexander Polynomial

The Alexander polynomial stands out as one of the earliest and most powerful tools for distinguishing between different types of knots. Introduced by J.W.

Alexander in 1928, this polynomial has since found its way into numerous applications that we discuss later on in Section 6.2. In this section, we will find that the Alexander polynomial is a useful, but not infallible, invariant.

**Definition 4.1** (Alexander Polynomial). The Alexander polynomial [8] of a knot in  $\mathbb{S}^3$  is defined by  $\Delta(t) = \det(V^T - tV)$ , where  $V$  is the Seifert matrix and  $V^T$  is the transpose of this matrix.

To make sense of this, we must introduce a new and essential concept in knot theory: the **Seifert surface**.

**Definition 4.2** (Seifert Surface). A Seifert surface,  $S$ , for a knot,  $K$ , is an oriented surface embedded in  $\mathbb{S}^3$  with the boundary of  $S$  being exactly the knot  $K$ .

In order for us to construct a Seifert surface, we must follow **Seifert's Algorithm** (first given in 1934) [9]:

1. Choose the orientation of a knot  $K$ .
2. Smooth every crossing admitting to orientation using the following moves: at each crossing, first identify the two **incoming strands** (the strands approaching the crossing) and the two **outgoing strands** (the strands leaving the crossing) before then eliminating the crossing itself by swapping which incoming strand connects to which outgoing strand. This obtains a set of non-intersecting closed curves called **Seifert circles**.
3. Fill in each Seifert circle to form a disc. We nest the discs at different heights perpendicular to the plane if some are enclosed within others. The nesting causes the  $z$ -coordinate to vary linearly.
4. Now, where the crossings originally were, we connect the disks using half-twisted bands to create an orientable surface with knot  $K$  as its boundary.

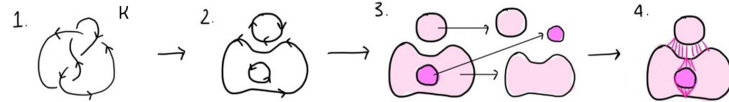


Figure 14: A figure-eight knot under Seifert's Algorithm.

Once we have constructed a Seifert surface,  $S_k$ , for a knot,  $K$ , we can then define the **Seifert matrix**,  $V = (v_{ij})$ . The entries of this matrix rely on a bilinear form known as the **Seifert form**,  $(v_{ij}) = lk(\alpha_i^+, \alpha_j^-)$ .

Here each  $\alpha_i$  represents a Seifert circle, with  $\alpha_i^+$  being the respective **push-off** of  $\alpha_i$ . To form the push-off, we move the curve  $\alpha_i$  slightly off the surface in the direction of the normal vector of  $\alpha_i$ . This creates a new curve that is parallel to  $\alpha_i$  but does not lie on the surface.

So when it comes to computing the linking number  $lk(\alpha_i^+, \alpha_j)$ , we look at the interactions between  $\alpha_i^+$  and  $\alpha_j$  and assign: +1 for a positive crossing, -1 for a negative crossing and 0 otherwise.

Now, we incorporate all we have learnt about the Alexander polynomial so far into the following example. This example uses work from [10].

**Example 4.1.** We start our example by considering a right-handed trefoil knot  $K$  and its respective Seifert surface  $S_K$ . While the diagram of the right-handed trefoil knot presented in the following Figure 15 does not look like what we see later on in Section 6.1, the two are in fact equivalent (this one has just been transformed).

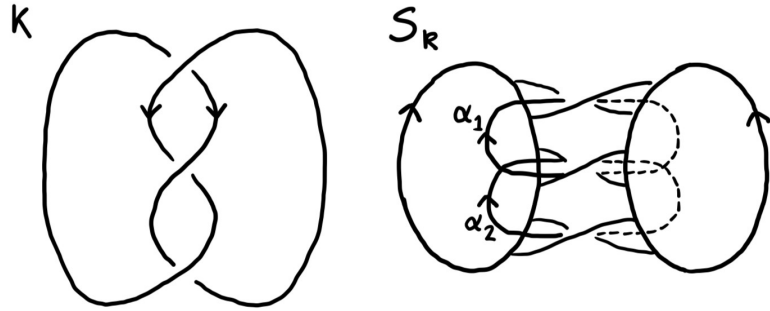


Figure 15: A right-handed trefoil knot  $K$  and its Seifert surface  $S_K$ .

As we can see, we have two closed curves  $\alpha_1$  and  $\alpha_2$  on the Seifert surface.

Now we consider our interactions between our curves  $\alpha_1, \alpha_2, \alpha_1^+$  and  $\alpha_2^+$  to form our linking numbers.

And so, for a right-handed trefoil knot our Seifert matrix is as follows:

$$V = \begin{pmatrix} lk(\alpha_1^+, \alpha_1) & lk(\alpha_1^+, \alpha_2) \\ lk(\alpha_2^+, \alpha_1) & lk(\alpha_2^+, \alpha_2) \end{pmatrix} = \begin{pmatrix} -1 & -1 \\ 0 & -1 \end{pmatrix}.$$

Recalling the definition of the Alexander polynomial  $\Delta(t) = \det(V^T - tV)$ , we can now substitute in our above value for  $V$  to obtain:

$$\begin{aligned}
\Delta(t) &= \det(V^T - tV) \\
&= \det \left( \begin{pmatrix} -1 & -1 \\ 0 & -1 \end{pmatrix}^T - t \begin{pmatrix} -1 & -1 \\ 0 & -1 \end{pmatrix} \right) \\
&= \det \left( \begin{pmatrix} -1 & 0 \\ -1 & -1 \end{pmatrix} - \begin{pmatrix} -t & -t \\ 0 & -t \end{pmatrix} \right) \\
&= \det \begin{pmatrix} -1+t & t \\ -1 & -1+t \end{pmatrix} \\
&= (-1+t)(-1+t) - (t)(-1) \\
&= (1-t-t+t^2) - (-t) \\
&= 1-2t+t^2+t \\
&= t^2-t+1 \text{ as the Alexander polynomial.}
\end{aligned}$$

## 4.2 The Jones Polynomial

The Jones polynomial is another fundamental invariant in knot theory, introduced by Vaughan Jones in 1984. This polynomial was groundbreaking because it could do something that the Alexander polynomial could not do reliably: distinguish mirror images of knots.

The definition of the Jones polynomial uses what is known as a **skein relation**, which describes how the polynomial changes as the knot diagram is modified locally.

**Definition 4.3.** (Skein Relation) To compute the Jones polynomial, we start by setting the initial condition that the Jones polynomial of the unknot is  $V_0 = 1$ .

Subsequently, we then apply a recursive relationship known as a skein relation. It is defined as:

$$\frac{1}{t}V_{D_+}(t) - tV_{D_-}(t) = \left(\sqrt{t} - \frac{1}{\sqrt{t}}\right)V_{D_0}(t),$$

where  $D_+$ ,  $D_-$ , and  $D_0$  represent three variations of a knot or link differing only in a single tangle (see Section 2.5). They are collectively referred to as a ‘skein triple,’ and are depicted as in Figure 16.

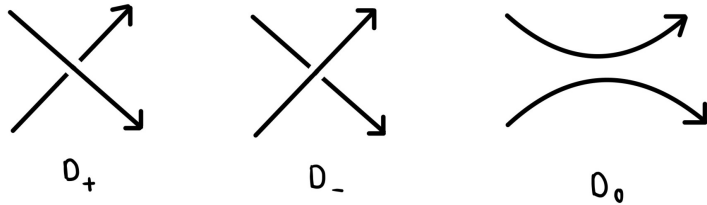


Figure 16: Conway’s Skein Triple

For clarity:

- $D_+$  is the diagram with a positive (right-handed) crossing,
- $D_-$  is the diagram with a negative (left-handed) crossing,
- $D_0$  is the smoothed version of the crossing, where the two incoming strands and the two outgoing strands have been reconnected without any crossing.

This recursive relationship is applied to reduce complex knots into simpler forms, ultimately leading to the Jones polynomial [11].

Given Definition 4.3, let us now emphasise the two main properties of the Jones polynomial: two equal links have the same Jones polynomial and the unknot has a Jones polynomial of value 1.

With these properties in mind, we present some examples to show how the skein relation suffices to calculate  $V_D(t)$  inductively on all links. This example will be a variation of the eponymous Vaughan Jones' work [12] with the end goal of calculating the Jones polynomial of the trefoil.

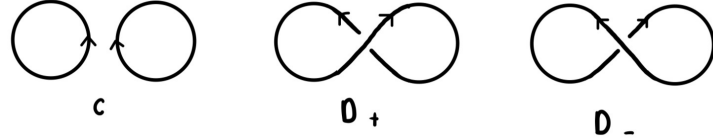


Figure 17: Unlinked circles with a skein relation.

We begin with two unlinked circles, which we have referred to as the link  $C$  in the above Figure 17. Also in Figure 17, we can see that  $D_+$  and  $D_-$  are able to be deformed by way of Reidemeister moves (see Section 3.1) into the unknot. Hence, we have  $V_{D_+} = V_{D_-} = 1$ .

Thus, using our recursive equation for the skein relation in Definition 4.3, we find that the Jones polynomial of  $C$  is:

$$\begin{aligned} \left(\frac{1}{t}\right)V_{D_+} - tV_{D_-} &= \left(\sqrt{t} - \frac{1}{\sqrt{t}}\right)V_C \\ \left(\frac{1}{t}\right) - t &= \left(\sqrt{t} - \frac{1}{\sqrt{t}}\right)V_C \\ V_C &= \frac{\left(\frac{1}{t}\right) - t}{\left(\sqrt{t} - \frac{1}{\sqrt{t}}\right)} \\ V_C &= -\left(\sqrt{t} + \frac{1}{\sqrt{t}}\right). \end{aligned}$$

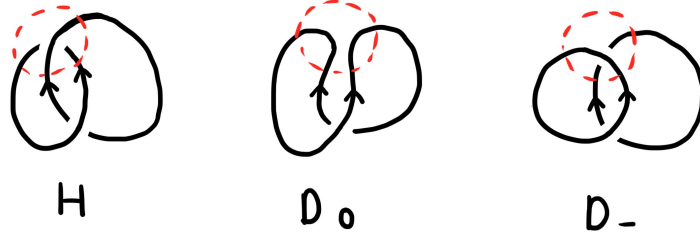


Figure 18: Hopf link with a skein relation.

Next, we move on to the Hopf link, which we have denoted as  $H$  in the above Figure 18.

Also in Figure 18, we are able to see that  $D_0$  is equivalent to the unknot. Hence, we have  $V_{D_0} = 1$ . To the right of our diagram for  $D_0$ , we then have what we can identify as being two unlinked circles denoted as  $D_-$ . From this, we therefore have:

$$V_{D_-} = V_C = -\left(\sqrt{t} + \frac{1}{\sqrt{t}}\right).$$

Thus, again using our recursive equation for the skein relation in Definition 4.3, we obtain the following Jones polynomial for  $H$ :

$$\begin{aligned} \left(\frac{1}{t}\right)V_H - tV_{D_-} &= \left(\sqrt{t} - \frac{1}{\sqrt{t}}\right)V_{D_0} \\ \left(\frac{1}{t}\right)V_H - t\left(-\left(\sqrt{t} + \frac{1}{\sqrt{t}}\right)\right) &= \left(\sqrt{t} - \frac{1}{\sqrt{t}}\right) \\ V_H &= t\left(\sqrt{t} - \frac{1}{\sqrt{t}}\right) - t^2\left(\sqrt{t} + \frac{1}{\sqrt{t}}\right) \\ V_H &= -\sqrt{t}(1 + t^2). \end{aligned}$$

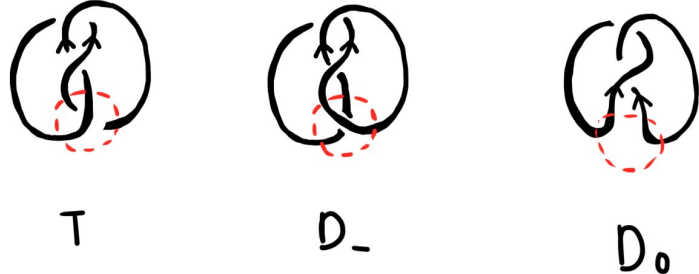


Figure 19: A right-handed trefoil with a skein relation.

Finally, we can use the previous two examples we have done to determine the Jones polynomial of a right-handed trefoil. Drawn the same as in Figure 15, we have denoted it as  $T$  in the above Figure 19.

Also in Figure 19, we can see that  $D_-$  is the unknot and that  $D_0$  is what our Hopf link  $H$  was. Hence, with  $V_{D_0} = V_H$ , we again use our recursive equation for the skein relation in Definition 4.3 and obtain the following Jones polynomial for our right-handed trefoil  $T$ :

$$\begin{aligned} \left(\frac{1}{t}\right)V_T - tV_{D_-} &= \left(\sqrt{t} - \frac{1}{\sqrt{t}}\right)V_{D_0} \\ \left(\frac{1}{t}\right)V_T - t &= \left(\sqrt{t} - \frac{1}{\sqrt{t}}\right)(-\sqrt{t}(1+t^2)) \\ \left(\frac{1}{t}\right)V_T - t &= (-t+1)(1+t^2) \\ \left(\frac{1}{t}\right)V_T &= 1+t^2-t^3 \\ V_T &= t+t^3-t^4. \end{aligned}$$

So, we now have two important tools for telling knots apart. While the Alexander and Jones polynomials are incredibly useful, they are not perfect and can still fail to distinguish some knots. In the next section, we will take a different approach by exploring knots from a topological perspective, uncovering new ways to understand and classify them.

## 5 Categorisation of Knots from a Topological Perspective

### 5.1 Torus Knots

**Torus knots** are a small family of knots, characterised by the property that they can be embedded on the surface of a standard torus in  $\mathbb{R}^3$ . First, we explain

what the motivation is for studying torus knots, how their embedding can be described, and the notation used when considering torus knots.

Every knot can be viewed in 3-space, with a projection in the plane which shows the crossings of a given knot. To consider subclasses of knots, we may take a subset of  $\mathbb{R}^3$  and consider which knots can exist in this space. Torus knots consider the subset of knots which exist on the surface of a torus without intersections. Unlike most other knots, torus knots can be easily classified.

Any torus knot can be described by the number of times it wraps around the meridian (the ‘short way’) and the longitude (the ‘long way’) of a torus, as illustrated in Figure 20 below.

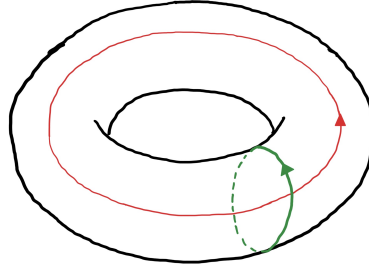


Figure 20: A torus with its meridian in green and longitude in red.

With  $p$  and  $q$  coprime, we use the convention  $(p, q)$  to describe a torus knot where:

$p$  = number of times a knot wraps around the meridian,

$q$  = number of times a knot wraps around the longitude.

If  $p$  and  $q$  are not coprime,  $(p, q)$  would instead construct a torus link with multiple components embedded on the standard torus.

Conveniently, any such  $(p, q)$  is a knot invariant (as in Definition 3.3): any two knots that can be embedded on the surface of a torus with the same  $p$  and  $q$  are the same knot, up to smooth deformation.

It can also be shown that all torus knots are prime knots [13], but proofs for both invariance and primality are beyond the scope of this report. Now though, let us move on to showing some basic torus knots:

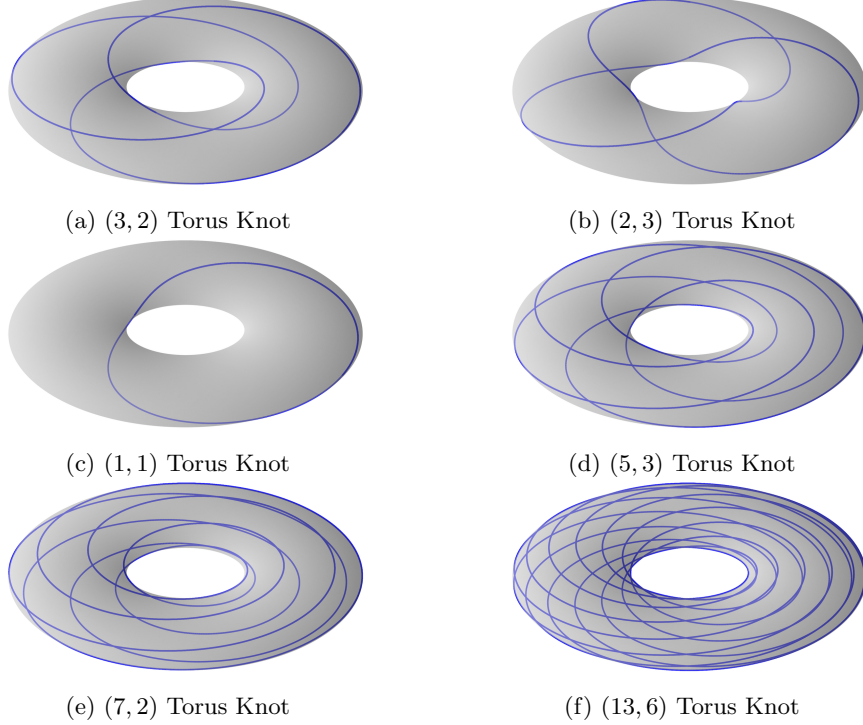


Figure 21: A selection of torus knots (see Appendix for the Python code that produced them).

## 5.2 Satellite Knots

Torus knots can be generalised naturally in two ways: we could consider knots embedded on the surface of objects with more than one hole (which topologists refer to as a **genus n-surface**), or we could consider embeddings on a non-standard torus. Both are relevant within knot theory, but the latter is regarded as more useful to knot theorists and such constructions are known as **satellite knots**.

Consider a knot  $K_1$  embedded within a standard torus  $T$ . Now, knot the torus  $T$  into the shape of a second knot, which we will refer to as  $K_2$ . As a result,  $K_1$  has now been changed to another knot and this will be referred to as  $K_3$ . This new knot,  $K_3$ , is called a satellite knot. In this construction, we refer to  $K_1$  as the **pattern knot** and to  $K_2$  as the **companion knot**.

For clarity, we will now consider a basic example of a satellite knot in the following Figure 22. Note the Reidemeister moves performed on the unknot.

We must ensure that the knot  $K_1$  passes through every meridional disk, and cannot be isotoped to avoid any disks, as then  $K_1$  could exist unchanged within the companion knot of  $K_2$ .

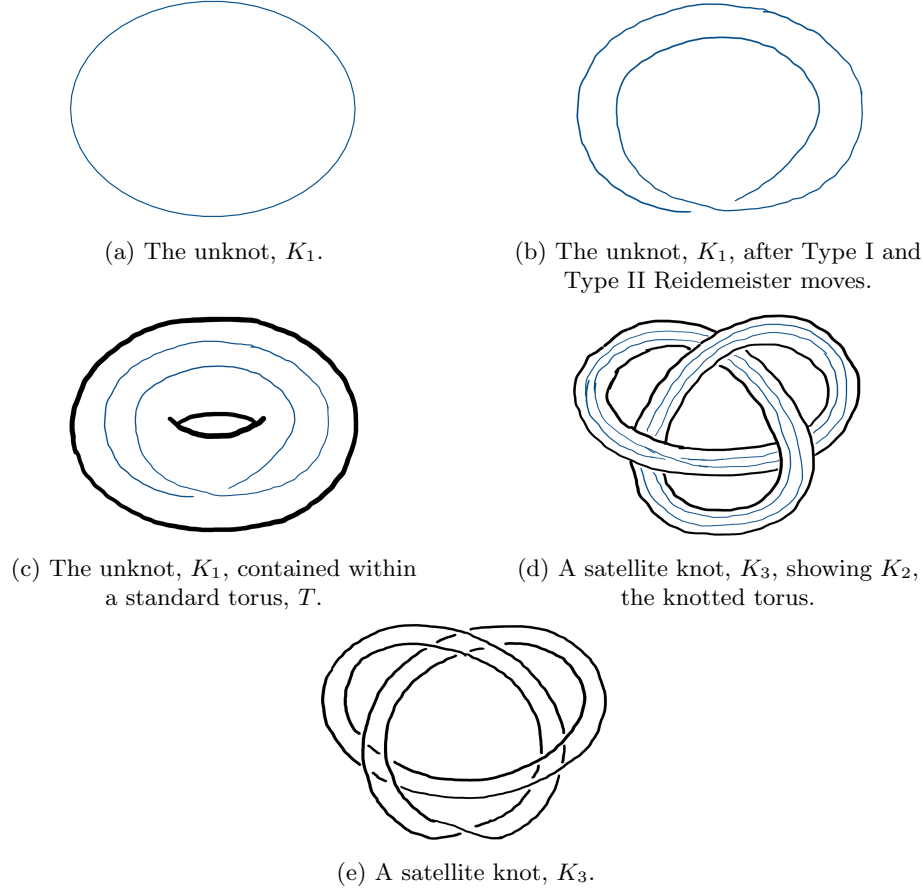


Figure 22: The satellite knot formed from the unknot with the trefoil as a companion knot.

Satellite knots can also be considered as a generalisation of composing two knots, a concept first seen in Section 2. In fact, if the pattern only has a single strand passing longitudinally around the torus,  $K_3$  is the composition of  $K_1$  and  $K_2$  (i.e.,  $K_3 = K_1 \# K_2$ ). In fact, similar to prime knots, every satellite knot can be obtained from a unique sequence of satellite knots. This was proven in 1987 by Soma [14], but the proof goes beyond the content of this report. Notably, the proof considers the pattern knot as the ‘preimage’ of a satellite knot for a given knotted torus, and constructs a sequence of preimage knots using a key invariant called the **Gromov invariant**.

One key example of a subset of satellite knots are **cable knots**. Cable

knots are formed by taking the pattern knot to be any torus knot  $(p, q)$  and can be intuitively understood as taking a cable and wrapping it around the companion knot,  $K_2$ , around the meridian  $p$  times and around the longitude  $q$  times. Cable knots are particularly useful in the field of algebraic geometry, which highlights the wide applications of knot theory in a variety of branches of modern mathematics.

### 5.3 Hyperbolic Knots

Hoste, Thistlewaite and Weeks [15] categorised every prime knot of fewer than 16 crossings, and found almost 2 million distinct prime knots. Interestingly, only 32 of these 2 million are torus or satellite knots. This prompts the question: what other families of knots are out there waiting to be discovered? Only one, in fact: hyperbolic knots.

In 1979, Thurston [16] proved that every prime knot is either a torus or satellite knot, or its knot complement is hyperbolic. Knots with this third property are known as **hyperbolic knots**. While torus and satellite knots can be explained, constructed, and tabulated with relative ease, hyperbolic knots are deeply entwined with hyperbolic geometry. We will briefly outline the process for understanding the key properties of these knots before providing an intuitive approach to considering the hyperbolic geometry of a familiar knot: the figure-eight knot.

Thus far, we have considered the properties of the knot itself, rather than the properties of the space the knot occupies. In hyperbolic knot theory, it is the complement of the knot that reveals interesting invariants. We will consider a knot  $K$  as occupying some 3-space,  $\mathbb{S}^3$ , denoting its complement (the space not occupied by our knot,  $K$ ) as  $\mathbb{S}^3 - K$ . The complement of the knot can then be described by a collection of tetrahedra connected by their edges. It is these tetrahedra that give rise to the key invariant of this family of knots: hyperbolic volume. At first glance, it may seem, intuitively, that any such hyperbolic tetrahedra would have infinite volume, but with careful construction and calculation using a hyperbolic metric, we can find a real, finite, hyperbolic volume for every knot with a complement in the 3-space.

Hyperbolic volume is an invariant of knots. If two knots have distinct hyperbolic volume, then they are distinct knots. Shown below are some knots and their respective hyperbolic volumes.

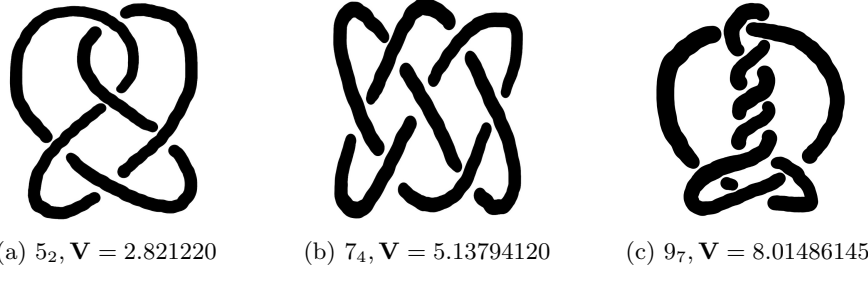


Figure 23: Some knots and their hyperbolic volumes,  $\mathbf{V}$  [1].

However, it is not the case that every knot has a distinct volume. For example, if a tangle in a hyperbolic knot is flipped (forming a mutant knot as in Definition 2.5), then the resulting hyperbolic volume will be unchanged. This represents a very small subset of hyperbolic knots, so in general, hyperbolic volume is an excellent way to distinguish knots. Since all hyperbolic knots have a real hyperbolic volume, we may consider which, if any, knot gives us the minimal volume. This was conjectured by Thurston in 1978, but was unproven until 2001. The proof, given in [17] by Cao and Meyerhoff, shows that the hyperbolic volume of the figure-eight knot to 5 decimal places is 2.02988 and is the minimal volume of any hyperbolic knot. Thus, the figure-eight knot can be considered as the simplest hyperbolic knot.

The process for determining the volume of a hyperbolic knot is completed numerically and is rarely computed by hand due to the complexities of hyperbolic tetrahedra. Instead, we will consider a non-rigorous, but intuitive, approach to determining the volume of a hyperbolic knot. This method is outlined by Purcell in [18]. In the following, we will consider the simplest hyperbolic knot, the figure-eight knot  $K = 4_1$ .

To begin, we will form a geometric intuition for the tetrahedra composing the complement of the figure-eight knot,  $\mathbb{S}^3 - K$ .

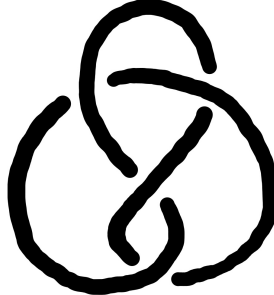


Figure 24: The figure-eight knot,  $K = 4_1$ .

Take the knot diagram in Figure 24 and consider inflating two balloons around the diagram: one ‘above’ the page, inflating downward toward the knot,

and a second ‘below’ the page, inflating upward. These balloons will touch in the regions defined by the knot diagram, and these regions will form the faces of our tetrahedra. At each crossing, two regions will share an edge, which can be thought of as corresponding to two sections of the same inflated balloon being separated by the particular crossing.

To help with our visualisation of this, we will simplify the knot diagram to include a point where each crossing was, and shaded faces for each balloon, as in the following Figure 25.

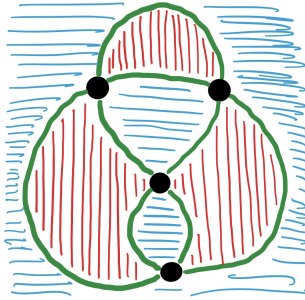


Figure 25: The shaded figure-eight knot with crossings reduced to a point. The red faces are formed by one balloon, and the blue faces by the other.

Taking the described faces and edges gives two tetrahedra. The volume of the knot complement can then be calculated by summing the area of the tetrahedra in hyperbolic space through  $n$  polynomials in  $n$  variables for  $n$  such tetrahedra, given by a hyperbolic metric. Such a metric ensures that the resulting volume is real.

Clearly, this approach is not rigorous and only gives a flavour of the process involved. A full explanation for finding the knot complement of the figure-eight knot, along with any other hyperbolic knot, in hyperbolic 3-space is given by Thurston in [19]. It forms part of the work for which he was awarded the Fields Medal in 1982.

## 6 Applications of Knot Theory Within Chemistry and Biology

Having now established the foundations of knot theory, it is natural for us to think about its real-world applications. Interestingly, knot theory provides us with a framework for understanding and analysing complex molecular structures, many of which exhibit knotted forms. This underlines why knot theory is able to find so many fascinating uses in a variety of fields, including in both chemistry and biology.

Take chemistry, for example: knotted molecules can be understood in two main contexts, as being either naturally occurring knots or synthesised knots.

Naturally occurring knots are seen in biological processes like protein folding, where proteins adopt complex topological structures essential to their function, and in DNA, which can form ‘knot’-like structures called i-motifs, with more than 50,000 of these structures found in the human genome alone [20].

Equally, it is possible to synthesise a molecule to have a knotted structure. For instance, chemists in 2017 from the University of Manchester synthesised the molecule below in Figure 26, known as the  $8_{19}$  knot, which, at the time, was the tightest physical structure yet discovered [21]. Since then, smaller and even more tightly knotted structures have been synthesised; notably, in 2024, the self-assembly of a trefoil-shaped ‘metallaknot’ was reported [22].

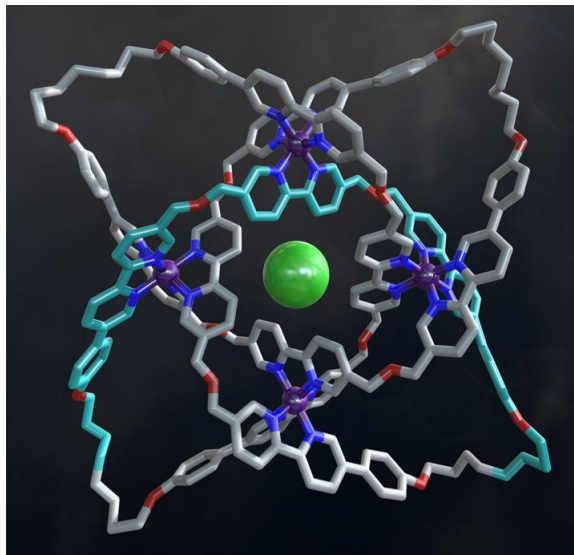


Figure 26: Crystal structure of a molecular  $8_{19}$  knot reported by Danon and coworkers in [21]. Image credit: Robert W. McGregor ([www.mcgregorfineart.com](http://www.mcgregorfineart.com)).

## 6.1 Molecular Chirality

In the world of molecular structures, **chirality** refers to the unique property possessed by certain objects that prevents them from being superimposed onto their own mirror images. Though we certainly have the capability to use all we have learned about knot theory so far to explore the structural complexity of molecules, we will instead place emphasis on their chirality and the different topological methods that we can use to analyse this characteristic.

At its core, chirality is probably best explained through the use of a simple analogy involving our hands. If we suppose we wish to look at the mirror image of the front of our left hand, we see in its reflection that we are still looking at the front of this same hand and not the right hand. Think about it: is it possible

for us to make our left hand into our right hand? Well, no, it is not. The best we can do is spin our hand around, but even then we only reveal its back and the back of a hand is definitely not the same as the front of a hand. Coined by Lord Kelvin, to be chiral therefore means to have this so-called '**handedness**' - the ability to distinguish between left and right.

With this in mind, we can begin to see just how naturally the concept of chirality fits into knot theory by introducing the following definition.

**Definition 6.1** (Chiral Knot). A chiral knot is defined as being 'a knot that is not capable of being continuously deformed into its own mirror image' [23].

If a knot is not chiral, it is instead termed **achiral** and can be continuously deformed into its own mirror image. Because of this, an achiral knot, being isotopic to its own mirror image, has no inherent 'handedness' about it.

But before we continue any further, it is important to address the terminology encountered in literature regarding achirality.

**Remark 6.2.** Amphichiral, amphiceiral, amphicheiral, achiral are all used interchangeably in literature on chirality. For consistency, we will use the term achiral.

We will now provide an example of an achiral knot: the figure-eight knot.

**Example 6.1.** To demonstrate that the figure-eight knot is an achiral knot, we deform it by way of the Reidemeister moves seen in Section 3.1.

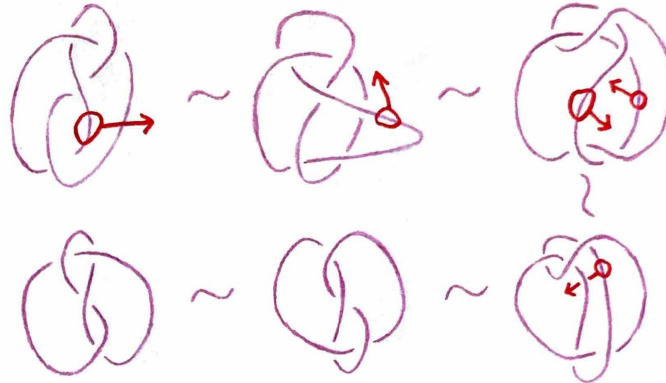


Figure 27: Working clockwise from the top-left, we continuously deform the  $4_1$  knot into its mirror image. In order to denote equivalence between each stage of deformation, we have used the  $\sim$  symbol.

In Figure 27, it is evident that when the figure-eight knot is mirrored, the crossings in the mirror image are exactly the reverse of what they are in the original. This is easy to spot in the centre of the knot since here the left strand goes over the right in the original, while the right strand goes over the left in the mirror image.

And, as Kauffman said, ‘the knot  $K^*$  obtained by reversing all the crossings of [a knot]  $K$  is called the mirror image of  $K$ ’ [24]. This confirms the figure-eight knot must be achiral, as it can be continuously deformed into its mirror image.

Interestingly, within the broader concept of chirality, a specific term does indeed exist to describe objects that can be continuously deformed into their mirror image: we call them **topologically achiral**. To fully understand this concept, it is just as important to define what it means to be its antonym of **topologically chiral**.

**Definition 6.3** (Topological Chirality). An object is said to be topologically chiral if (assuming complete flexibility) it is not possible for it to be deformed into its mirror image. Otherwise, it is said to be topologically achiral (a property illustrated in Example 6.1).

Taking a different knot from the catalogue of key knots seen in Section 2.2, let us see how this definition applies in practice by way of an example.

**Example 6.2.** Having chosen the trefoil knot of Image 1b in Figure 1, we start this example by drawing the knot as well as its mirror image.

To do so, we follow Kauffman’s aforementioned advice of drawing it so all the crossings are the reverse to what they originally are and thus obtain the following knot diagrams.



Figure 28: The trefoil knot alongside its mirror image.

While in Example 6.1 we were able to show the figure-eight knot was equivalent to its mirror image under Reidemeister moves, we can see that this simply will not be possible here: these two trefoil knots are not equivalent. Not only does this tell us that the trefoil knot is topologically chiral, it also tells us of the existence of a left-handed trefoil (on the left of Figure 28) and a right-handed trefoil (on the right of Figure 28).

**Remark 6.4.** Returning to our catalogue of key knots in Figure 1, we are able to categorise each of them. The unknot and the figure-eight knot are topologically achiral, as is the  $6_3$  knot. The trefoil knot, the  $5_1$  knot, the  $5_2$  knot, the  $6_1$  knot, and the  $6_2$  knot are topologically chiral.

Notably, another example of a topologically achiral knot is the **composite square knot**, which is formed by combining two trefoil knots with opposing

handedness [25]. And if we are to recall our definition of tricolourability (Definition 3.4), we can even say that this knot is tricolourable too.

**Example 6.3.** To aid us in our explanation, we will first draw both the left-handed and right-handed trefoil coloured before taking their connected sum (as in Definition 2.2).

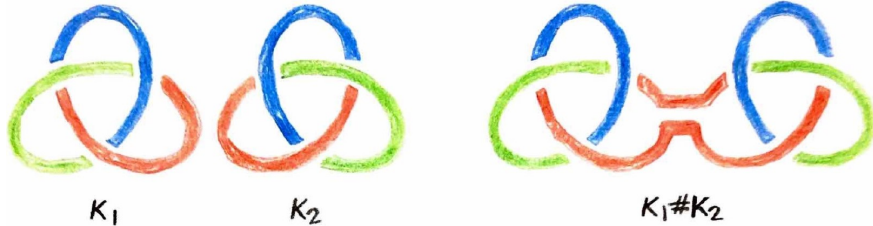


Figure 29: From left to right, we have the right-handed trefoil knot  $K_1$ , the left-handed trefoil knot  $K_2$ , and the composite square knot  $K_1 \# K_2$ .

Having found the trefoil knot to be tricolourable in Example 3.2, the above Figure 29 shows we are able to take the connected sum of the right-handed trefoil  $K_1$  and the left-handed trefoil  $K_2$ , and find that the resulting composite square knot  $K_1 \# K_2$  retains tricolourability.

But, the same cannot be said for the trefoil knot's topological chirality. With  $K_1 \# K_2$  noticeably possessing 'a plane of symmetry where the knots are joined' [26], it maps onto itself by reflection across this plane. As a result, this thereby confirms the composite square knot to be topologically achiral.

After Example 6.3, it should now be more apparent than ever just how embedded a concept topological chirality is in the world of knot theory. But while topological chirality is the most important subclass of chirality for knot theorists, the rest of the world arguably places far greater emphasis on **chemical chirality**: specifically, the determining of whether a molecule is chemically chiral or achiral, as this distinction is critical in understanding a drug's pharmacological properties.

**Definition 6.5** (Chemical Chirality). A molecule is said to be chemically chiral if it is not possible for it to transform itself to its mirror image. Otherwise, it is said to be chemically achiral.

Here, it is important to note that the term 'transform' in Definition 6.5 refers to the ability of a molecule's chemical structure to move certain parts around while leaving the overall structure unchanged, meaning that parts of the molecule could even be spun around without altering the molecule as a whole. This stresses the crucial distinction between chemical chirality and chemical achirality. Highlighting this distinction is essential as it is fundamental in determining how molecules interact, especially in chemical and biological systems.

Also key to determining how molecules interact is the presence of **chiral environments**; spatial arrangements in which the distribution of parts does not have an internal plane of symmetry [27].

According to [28], it is known that ‘the **enantiomers** of a chiral drug may vary in their interactions with chiral environments such as enzymes, proteins, receptors, etc of the body.’ Much like how we defined a chiral knot in Definition 6.1, an enantiomer is simply one of a pair of molecules which are non-superimposable mirror images of each other. And so, with enantiomers having the potential to interact differently with these chiral environments, it can often be the case that while one enantiomer turns out to be therapeutically beneficial, the other is inactive and/or potentially harmful [29]. Thus, this danger makes clear exactly why pharmaceutical companies care so much about this particular subclass of chirality.

To see this in practice, we will now provide examples of the two contrasting molecules of limonene and thalidomide.

**Example 6.4.** First, we will present the chiral forms of limonene.

Depending on which enantiomer we encounter, it is important to remember that they are chemically identically despite how unbelievable this might be with their differences in how they interact with biological systems and light.

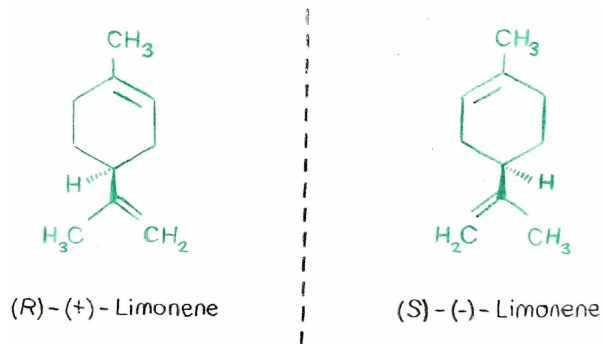


Figure 30: The enantiomers of limonene,  $(R)$  –  $(+)$ –Limonene and  $(S)$  –  $(-)$ –Limonene. For an explanation on the notation used, see [29].

The enantiomers in Figure 30 serve distinct purposes based on their chiral configuration. The more common  $(R)$  –  $(+)$ –Limonene is used in cleaning products as a fragrance compound and as a dispersing agent for oils, while the less common  $(S)$  –  $(-)$ –Limonene can be found in many essential oils.

Interestingly, these enantiomers both possess a citrus-like scent: we have  $(R)$  –  $(+)$ –Limonene with a scent of oranges and  $(S)$  –  $(-)$ –Limonene with a scent of lemons [30]. Either way, the impact of their chirality is harmless.

**Example 6.5.** For contrast with Example 6.4 above, we will now present the chiral forms of thalidomide.

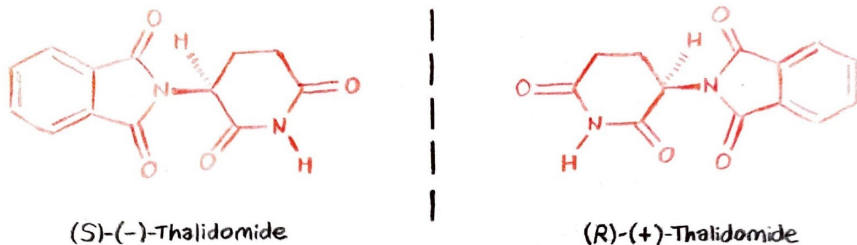


Figure 31: The enantiomers of thalidomide,  $(S) - (-)$ -Thalidomide and  $(R) - (+)$ -Thalidomide. Again, [29] provides an explanation on the notation used.

Thalidomide was a drug widely prescribed to pregnant women for nausea in the late 1950s and early 1960s. It was sold as a 50 : 50 mixture of both enantiomers.

Depicted on the right in Figure 31, the  $(R) - (+)$ -Thalidomide enantiomer was found to act as a sedative and antidepressant with very few side-effects while effectively helping to fight nausea as intended. However, its mirror image  $(S) - (-)$ -Thalidomide was **teratogenic**, causing severe birth defects like phocomelia [31].

Worldwide, it is estimated that thousands of children were born with thalidomide-associated deformities [32]. As a result, pharmaceutical companies have since enacted tighter drug testing and side-effect reporting policies, while also considering the implications of molecular chirality in their products.

## 6.2 Protein Folding

Proteins are built as open-folded chains of amino acids. Although the precise mechanics of folding and knotting are yet unknown, we know that these processes provide vital structure and function to proteins.

Five proteins, or indeed five knots, have been discovered in the Protein Data Bank (PDB, [33]) that can fold.

**Observation.** As of the current moment, only five different types of knot have been identified in proteins in the Protein Data Bank (see [34], [35] and [36] for an in-depth exploration of the knotting complexity of proteins and insights into why exactly so few knot types have been able to be identified).

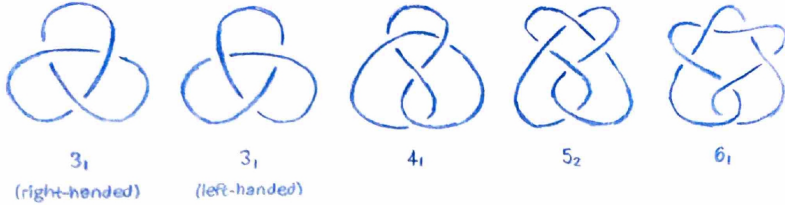


Figure 32: The five knots found in proteins, consisting of both the trefoil knot and its mirror image, the figure-eight knot ( $4_1$ ), one view of the  $5_2$  knot, and one view of the  $6_1$  knot.

From Figure 32, we might now be wondering how we study these structures. Researchers have looked at protein knotting from a variety of different angles, including via experimental techniques, computational simulations, and theoretical modelling.

One known model is the Flapan et al. Model (2019) [37]. According to this model, there are eight possible configurations of what a knotted protein can look like, each capable of representing any protein knot within these predefined categories.

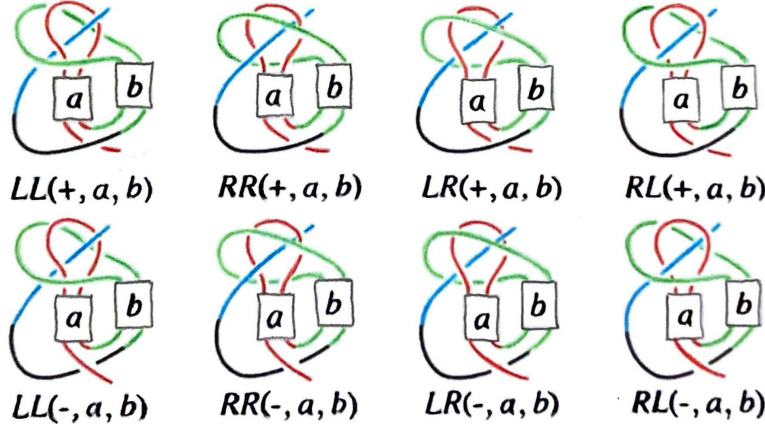


Figure 33: The Flapan et al. Model outlines the potential templates for knotted protein configurations using a set of parameters.

Furthermore, this model encompasses every knot that has been found so far and aligns with the observed probabilities of different knot types [38]. Additionally, the model predicts the existence of certain knots that have yet to be observed in proteins but could potentially emerge in future findings, these configurations are considered the most likely candidates of ones that would show up, though this is hypothesised.

This is where classical knot theory reaches an impasse. Its limitations open the door to the concept of virtual knots. By introducing a third type of crossing known as a **virtual crossing**, we can expand upon the Flapan et al. Model, allowing for a broader representation of knotted forms and providing a framework to account for the more intricate configurations of proteins.



Figure 34: A virtual crossing between two crossings.

**Definition 6.6** (Virtual Knot). A virtual knot is a generalisation of a classical knot [39] that includes a third crossing type: virtual. As shown in Figure 34, we represent a virtual crossing by way of two crossing segments and a circle encircling their vertex [40].

Introduced by Kauffman in 1998, the relatively new concept of virtual knots is an extension of classical knot theory that incorporates a third type of crossing, represented by a circle, to indicate an ambiguous crossing. Unlike the usual over-crossings and under-crossings, this ambiguous crossing is deliberately indeterminate; we do not know which strand passes over or under the other. Think of Schrödinger’s cat: just as the cat is simultaneously alive and dead, a virtual crossing embodies both over and under possibilities.

In Section 3.1, we first introduced the concept of Reidemeister moves which now proves to be adaptable within this new framework of virtual knots. Specifically, we can incorporate the virtual crossing type into the existing set of allowable moves in Definition 3.1. Thus, just as the Reidemeister moves we were previously aware of apply to over-crossings and under-crossings, virtual Reidemeister moves apply to virtual crossings. In Figure 35 below, we will demonstrate these moves, highlighting how Reidemeister’s framework accounts for the ambiguity of virtual crossings, preserving knot invariants (Definition 3.3).

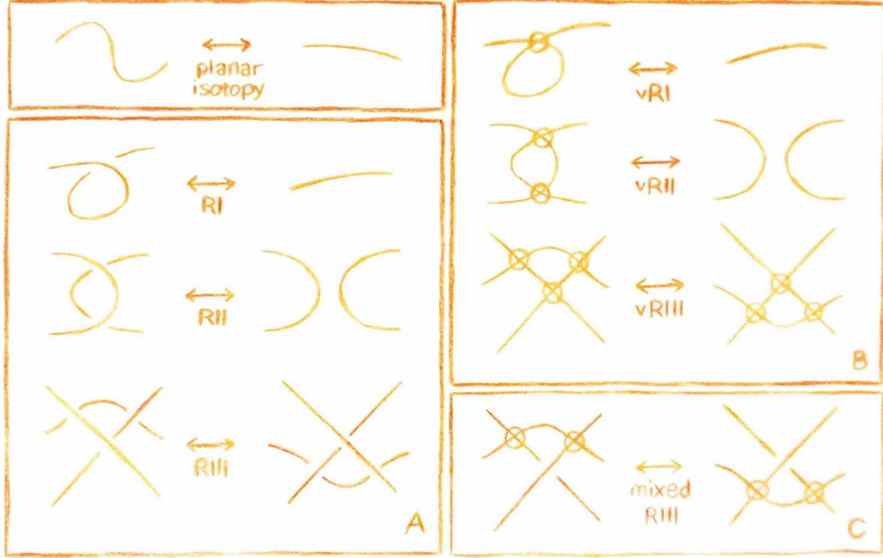


Figure 35: Together with an example of a planar isotopy move in the top-left (defined earlier in Section 3), the transformations shown here in images A, B, and C, respectively, are the classical Reidemeister moves revisited from Figure 6, the virtual Reidemeister moves, and a mixed Reidemeister move.

In fact, being able to extend Reidemeister moves to virtual crossings in this way allows us to manipulate virtual knots while still preserving their topological structure. This framework has proven to be particularly useful in the study of biological structures.

For instance, let us consider the structure of an open protein chain. In this context, when we attempt to make it into a closed structure (in a step towards trying to eventually analyse its knotting), we face a challenge: the exact path by which the chain might close is inherently indeterminate. As a result, this means it is impossible for us to obtain the precise crossing information we are looking for. To account for this ambiguity, we treat these crossings as virtual, thereby allowing us to look at proteins as virtual knots.

**Observation** (Alexander et al. (2017) [41]).

- Introduced a new method for resolving knotting in open protein chains using virtual knots.
- Virtual crossings capture the topological ambiguity in closing the open chains.

To see Alexander et al. in action, we will now present an example.

**Example 6.6.** Here, we have a protein chain that we want to make a closed structure. How are we going to do this?



Figure 36: On the left is the open chain we are trying to resolve knotting in. To do so, Alexander et al. tells us we can use virtual knots and so on the right is our open chain represented as a virtual knot.

With one way being for the strand to go underneath and another way being for it to go on top, Figure 36 demonstrates to us a virtual crossing. This virtual crossing does in fact make a difference.

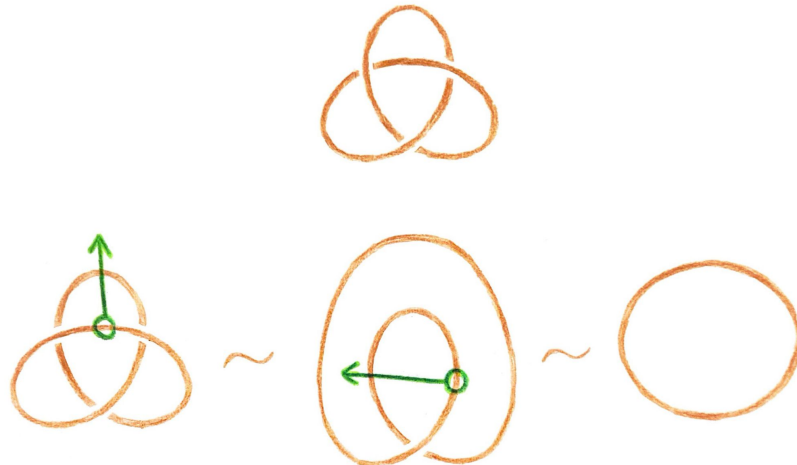


Figure 37: Evidently, the over-crossing turns out to be the left-handed trefoil knot. Working left to right, we are then able to continuously deform the under-crossing into the unknot by way of Reidemeister moves.

When researchers then applied Alexander et al's proposed method to real protein folding data, they were able to find that virtual knots do indeed appear in open protein chains. As of now, the following virtual knots illustrated in Figure 38 have been identified alongside a small number of other virtual knots. Due to limitations with the work of Jeremy Green and his table of virtual knots [42], it remains a challenge to figure out what these additional virtual knots are.

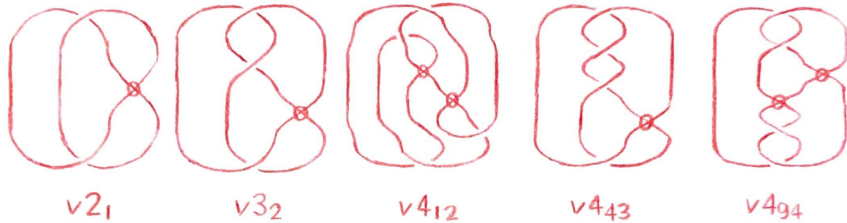


Figure 38: The five virtual knots currently identified in open protein chains.

Interestingly, what stands out in Figure 38 is the relatively low number of virtual crossings in each of the virtual knots. With only one or two virtual crossings at most across the knots, this observation seems like it should tell us something about the structural patterns of protein chains and yet there has been little research to confirm whether this is indeed the case. However, [43] does give us some hope, suggesting that ‘viewing the knot ‘virtually’ offers a more subtle understanding of [a] protein molecule’s shape,’ providing insights that classical knots may otherwise overlook. This idea is supported by the fact that virtual knot types are more natural than classical knot types are [44], as they do not have to close. This has opened up new avenues for further research, such as understanding how exactly virtual knots contribute to protein structure and function.

## 7 Conclusion

Knot theory is a varied field of mathematics. With beginnings in classical physics, knots are an exciting area of topology and are now integral to molecular chemistry. In modern knot theory, tabulation is ongoing, and new invariants continue to categorise our widening understanding of knots. We direct interested readers to Cromwell’s *Knots and Links* [45] for a broader understanding of knot theory and its place in topology, and recommend *Machine Learning of Knot Topology in Non-Hermitian Band Braids* by Chen et al. [46] to explore the frontier of mathematical knots. New discoveries in knot theory are shaping both the mathematical and physical worlds around us, with the future of topology tied up in knots.

## References

- [1] C. C. Adams. *The Knot Book: An Elementary Introduction to the Mathematical Theory of Knots*. American Mathematical Society, Providence, 2004.
- [2] J. W. Alexander and G. B. Briggs. On types of knotted curves. *Annals of Mathematics*, 28(1/4):562–586, 1926–1927.
- [3] P. G. Tait. *On knots I, II, III, Scientific Papers, Vol. I*. Cambridge University Press, Cambridge, 1898.
- [4] K. Reidemeister. Elementare begründung der knotentheorie. *Abhandlungen aus dem Mathematischen Seminar der Universität Hamburg*, 5(1):24–32, December 1927. In German.
- [5] S. Dixon. Composite knot determinants. *Lecture note*, 2010. Available at <https://www.math.uchicago.edu/~may/VIGRE/VIGRE2011/REUPapers/Dixon.pdf> (Accessed: 5 November 2024).
- [6] B. Ryan. Math5004m: Knot theory. Master’s thesis, University of Leeds, May 2020. Available at <https://bradjackryan.github.io/Files/Knot-Theory.pdf> (Accessed: 5 November 2024).
- [7] C. Livingston. *Knot Theory*. Carus Mathematical Monographs. Mathematical Association of America, Washington, D.C., 1993.
- [8] E. W. Weisstein. Alexander polynomial. From MathWorld—A Wolfram Web Resource. Available at <https://mathworld.wolfram.com/AlexanderPolynomial.html> (Accessed: 12 November 2024).
- [9] J. Collins. An algorithm for computing the seifert matrix of a link from a braid representation. *Ensaios Matemáticos*, 30(4), November 2007.
- [10] K. Murasugi. *Knot Theory and Its Applications*. Modern Birkhäuser Classics. Birkhäuser, Boston, 1996.
- [11] J. H. Przytycki et al. *Lectures in Knot Theory: An Exploration of Contemporary Topics*. Universitext. Springer, Cham, 2024.
- [12] V. Jones. The jones polynomial for dummies. *Lecture note*, 2014. Available at <https://math.berkeley.edu/~vfr/jonesak1.pdf> (Accessed: 14 November 2024).
- [13] G. Burde, H. Zieschang, and M. Heusener. *Knots*. De Gruyter, Boston, 2013.
- [14] T. Soma. On preimage knots in  $s^3$ . *Proceedings of the American Mathematical Society*, 100(3):589–592, July 1987.

- [15] J. Hoste, M. Thistlethwaite, and J. Weeks. The first 1,701,936 knots. *The Mathematical Intelligencer*, 20:33–48, January 2014.
- [16] W. P. Thurston. The geometry and topology of 3-manifolds. *Lecture note*, 1978. Available at <https://homepages.math.uic.edu/~kauffman/Thurston.pdf> (Accessed: 31 October 2024).
- [17] C. Cao and G. Meyerhoff. The orientable cusped hyperbolic 3-manifolds of minimum volume. *Inventiones Mathematicae*, 146:451–478, January 2001.
- [18] J. S. Purcell. Hyperbolic knot theory. *arXiv preprint arXiv:2002.12652*, 209, February 2020.
- [19] W. P. Thurston. Three dimensional manifolds, kleinian groups and hyperbolic geometry. *Bulletin (New Series) of the American Mathematical Society*, 6:357–381, May 1982.
- [20] C. D. Peña Martinez et al. Human genomic dna is widely interspersed with i-motif structures. *The EMBO Journal*, 43(20):4786–4804, August 2024.
- [21] J. J. Danon et al. Braiding a molecular knot with eight crossings. *Science*, 355(6321):159–162, January 2017.
- [22] Z. Li et al. Self-assembly of the smallest and tightest molecular trefoil knot. *Nature Communications*, 15(1):154, January 2024.
- [23] E. W. Weisstein. Chiral knot. From *MathWorld—A Wolfram Web Resource*. Available at <https://mathworld.wolfram.com/ChiralKnot.html> (Accessed: 14 November 2024).
- [24] L. H. Kauffman. An introduction to knot theory. In R. L. Ricca, editor, *An Introduction to the Geometry and Topology of Fluid Flows*, volume 47 of *NATO Science Series*, pages 77–104. Springer, Dordrecht, 2001.
- [25] S. L. Woltering. *Metal Template Synthesis of Novel Interlocked Architectures*. PhD thesis, University of Manchester, August 2017. Available at [https://pure.manchester.ac.uk/ws/portalfiles/portal/60828688/FULL\\_TEXT.PDF](https://pure.manchester.ac.uk/ws/portalfiles/portal/60828688/FULL_TEXT.PDF) (Accessed: 20 November 2024).
- [26] S. D. P. Fielden, D. A. Leigh, and S. L. Woltering. Molecular knots. *Angewandte Chemie International Edition*, 56(37):11166–11194, May 2017.
- [27] J. V. L. E. Xuan. Chiral environments: Sometimes, the environment shapes you. Stereochemistry blog, October 2018. Available at <https://blogs.ntu.edu.sg/cy1101-1819s1-g09/2018/10/chiral-environments/> (Accessed: 20 November 2024).
- [28] L. A. Nguyen, H. He, and C. Pham-Huy. Chiral drugs: an overview. *International Journal of Biomedical Science*, 2(2):85–100, June 2006.

- [29] J. McConathy and M. J. Owens. Stereochemistry in drug action. *Primary Care Companion to the Journal of Clinical Psychiatry*, 5(2):70–73, April 2003.
- [30] J. Isac-García et al. *Experimental Organic Chemistry: Laboratory Manual*. Elsevier, Amsterdam, 2016.
- [31] N. Vargesson. Thalidomide-induced teratogenesis: history and mechanisms. *Birth Defects Research Part C: Embryo Today*, 105(2):140–156, June 2015.
- [32] J. H. Kim and A. R. Scialli. Thalidomide: the tragedy of birth defects and the effective treatment of disease. *Toxicological Sciences*, 122(1):1–6, April 2011.
- [33] wwPDB consortium. Protein data bank: the single global archive for 3d macromolecular structure data. *Nucleic Acids Research*, 47(D1):D520–D528, October 2018.
- [34] P. Dabrowski-Tumanski et al. Knotprot 2.0: a database of proteins with knots and other entangled structures. *Nucleic Acids Research*, 47(D1):D367–D375, December 2018.
- [35] M. Jamroz et al. Knotprot: a database of proteins with knots and slipknots. *Nucleic Acids Research*, 43(D1):D306–D314, October 2014.
- [36] J. Sulkowska et al. Conservation of complex knotting and slipknotting patterns in proteins. *Proceedings of the National Academy of Sciences*, 109(26):E1715–E1723, June 2012.
- [37] E. Flapan, A. He, and H. Wong. Topological descriptions of protein folding. *Proceedings of the National Academy of Sciences of the United States of America*, 116:9360–9369, April 2019.
- [38] E. Tibor et al. Performance of the uniform closure method for open knotting as a bayes-type classifier. *arXiv preprint arXiv:2011.08984*, November 2020.
- [39] C. W. Ashley. *The Ashley Book of Knots*. Doubleday, New York, 1944.
- [40] L. H. Kauffman. Virtual knot theory. *European Journal of Combinatorics*, 20:663–691, November 1998.
- [41] K. Alexander, M. Dennis, and A. Taylor. Proteins analysed as virtual knots. *Scientific Reports*, 7:43200, February 2017.
- [42] J. Green. A table of virtual knots, 2004. Available at <https://www.math.toronto.edu/drorbn/Students/GreenJ/> (Accessed: 29 October 2024).
- [43] University of Bristol. New research shows that proteins are 'virtually' knotted. *Press release*, February 2017. Available at <https://www.bristol.ac.uk/news/2017/february/proteins-are-virtually-knotted-.html> (Accessed: 29 October 2024).

- [44] V.O. Manturov and I.M. Nikonov. Flat-virtual knot: introduction and some invariants. *arXiv preprint arXiv:2406.12864*, March 2024.
- [45] P. R. Cromwell. *Knots and Links*. Cambridge University Press, Cambridge, 2004.
- [46] J. Chen et al. Machine learning of knot topology in non-hermitian band braids. *Communications Physics*, 7(1), June 2024.

## Appendix

### Visualising Torus Knots

The following Python script was used to generate the depictions of the torus knots given in Figure 21.

```
1 import numpy as np
2 import matplotlib.pyplot as plt
3 from mpl_toolkits.mplot3d import Axes3D
4 def torus_knot(p,q):
5     # Parameters for the torus
6     R = 1 # Major radius of the torus
7     r = 0.5 # Minor radius of the torus
8
9     # Generate torus surface
10    u = np.linspace(0, 2 * np.pi, 1000)
11    v = np.linspace(0, 2 * np.pi, 500)
12    u, v = np.meshgrid(u, v)
13    x_torus = (R + r * np.cos(v)) * np.cos(u)
14    y_torus = (R + r * np.cos(v)) * np.sin(u)
15    z_torus = r * np.sin(v)
16
17    # Generate the torus knot on the surface
18    theta = np.linspace(0, 2 * np.pi, 10000)
19    x_knot = (R + r * np.cos(q * theta)) * np.cos(p * theta)
20    y_knot = (R + r * np.cos(q * theta)) * np.sin(p * theta)
21    z_knot = r * np.sin(q * theta)
22
23    fig = plt.figure(figsize=(10,10))
24    ax = fig.add_subplot(111, projection='3d')
25
26    # Plot torus
27    ax.set_box_aspect([2,2,0.2])
28    ax.grid(False)
29    ax.set_axis_off()
30    ax.plot_surface(x_torus, y_torus, z_torus, color='lightgrey',
31                    alpha=0.4, rstride=3, cstride=3, edgecolor='none')
32
33    # Plot torus knot
34    for i in range(len(x_knot) - 1):
35        linestyle = (0, (5,100000)) if z_knot[i] < 0 else 'solid'
36        # Dashed for z < 0
37        ax.plot(x_knot[i:i+2], y_knot[i:i+2], z_knot[i:i+2], color=
38                'b', lw=2, linestyle=linestyle)
39
40    filename = f"torus_knot_p{p}_q{q}.png"
41    plt.subplots_adjust(left=0, right=1, top=1, bottom=0)
42    plt.savefig(filename, format="png", dpi=300, bbox_inches='tight',
43                pad_inches=0)
44 p_q_vals = [(2,3), (3,2), (1,1), (5,3), (7,2), (13,6)]
45 for p, q in p_q_vals:
46     torus_knot(p,q)
```